This is an *Accepted Manuscript*, which has been through the Royal Society of Chemistry peer review process and has been accepted for publication.

Accepted Manuscripts are published online shortly after acceptance, before technical editing, formatting and proof reading. Using this free service, authors can make their results available to the community, in citable form, before we publish the edited article. We will replace this *Accepted Manuscript* with the edited and formatted *Advance Article* as soon as it is available.

You can find more information about *Accepted Manuscripts* in the **Information for Authors**.

Please note that technical editing may introduce minor changes to the text and/or graphics, which may alter content. The journal's standard **Terms & Conditions** and the **Ethical guidelines** still apply. In no event shall the Royal Society of Chemistry be held responsible for any errors or omissions in this *Accepted Manuscript* or any consequences arising from the use of any information it contains.

Journal Name

COMMUNICATION

A responsive MOF nanocomposite for decoding volatile organic compounds

You Zhou,[a] Bing Yan*[a]

A responsive luminescent MOF nanocomposite is developed by postsynthetic incorporation of Eu^{3+} cations into a robust nanocrystalline framework. The resulted MOF nanocomposite can serve as a platform for recognizing aromatic VOCs with simliar strucures and physical properties based on a unprecedented dual-readout identification scheme.

Luminescence metal-organic frameworks (MOFs) featuring permanent, well defined porosity and intense fluorescence have attracted great interest due to their potential application in light-emitting devices,[1] chemical sensing,[2] biomedicine[3] and barcoding.[1b,4] Among these applications, luminescent MOFs demonstrate particular potential in chemical sensing. This is because (1) the luminescence properties of MOFs are very sensitive to their structure characteristics, coordination environment of metal ions, and their interactions with guest species (such as coordination bonds, and π-π interactions and hydrogen bonding etc.), which provides the solid rationale for chemical sensing; (2) the structural and chemical tunability of MOFs produce their high selective recognition for analytes through pore sieving functions with diverse pore sizes or specific the interactions between the framework and analytes; (3) the high internal surface areas of MOFs and host framework-guest interactions may result in pre-concentration of analytes, thus giving rise to low detection limits and high sensing sensitivity.

In the past few years, chemical sensors based on luminescence MOFs have been widely investigated to detect metal cations,[5] anions,[6] small molecules,[7] gases,[8] temperatures,[9] pH values[10] and moisture,[11] which makes luminescence MOFs an important member in the club of 'smart materials'. The sensing function of volatile organic compounds (VOCs) has also been achieved in luminescence MOFs, and gained increasing attentions.[12] VOCs, such as aromatic species, are considered as a major group of toxic atmospheric pollutants. They present in indoor/outdoor air, as a consequence of the release from chemical industries, cosmetics, building blocks, etc. Therefore, effective detection of VOCs is of great importance both for environmental and health issues. However, most of these MOF fluorescence sensors explored thus far detect a single target compound from among several analytes, but can hardly differentiate targets from one another. Such MOF sensors commonly relied on guest-dependent luminescence intensity of one transition, which accuracy is susceptible to errors introduced by optical occlusion, concentration inhomogeneities, or excitation power fluctuations, thus greatly limits the capability in fine distinguishing chemical species with similar structures and physical properties.

In this work, we developed a responsive luminescence MOF nanocomposite by postsynthetic incorporation of Eu^{3+} cations into a robust nanocrystalline framework, which can serve as a platform for the recognition of aromatic VOCs with similar structures and physical properties, even homologues and isomers. The photoluminescence properties of the MOF nanocomposite highly depend on the guest aromatic volatile organic compounds (VOCs). Once the MOF composite accommodates a class of VOCs, identities regarding these VOCs can be recognized with characteristic different two-dimensional (2D) readouts which combine ratiometric emission intensity and luminescence quantum yield. Compared with the conventional emission intensity-based method for chemical sensing, the unprecedented dual-readout orthogonal identification scheme demonstrated here is expected to be more reliable and powerful as it is capable of maximizing the available information.

The robust parented framework $Zr_6(\mu^3\text{-}O)_4(OH)_4(bpy)_{12}$ (known as bpy-UiO, bpy = 2,2-bipyridine-5,5-dicarboxylic acid) was synthesized via a solvothermal reaction between $ZrCl_4$ and bpy ligand in the presence of DMF and glacial acetic acid. The product was then activated by Soxhlet extraction in methanol and dried under vacuum overnight to yield the fully desolvated bpy-UiO. Powder X-ray diffraction (PXRD) pattern of the resulted white solid was well matched with that simulated from the single crystal structure (Figure 1b).[13] The transmission electron microscopy (TEM) result revealed that the product consists of homogeneous particles with

a. Shanghai Key Lab of Chemical Assessment and Sustainability, Department of Chemistry, Tongji University, Siping Road 1239, Shanghai 200092, China. E-mail: byan@tongji.edu.cn;
† Electronic Supplementary Information (ESI) available. See DOI: 10.1039/b000000x/

COMMUNICATION

Journal Name
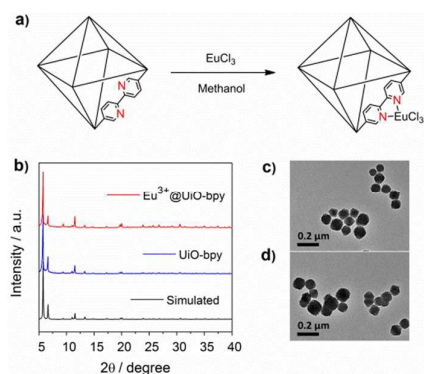
Figure 1 (a) Schematic illustration of the postsynthetic functionalization of UiO-bpy with Eu³⁺. (b) PXRD patterns of that simulated from the CIF file[13] (black), pristine UiO-bpy (blue), and Eu³⁺@UiO-bpy (red). (c), (d) Typical TEM image of nanocrystalline UiO-bpy and Eu³⁺@UiO-bpy, respectively.

Figure 2 Room-temperature photoluminescence spectra of (a) UiO-bpy and (b) Eu³⁺@UiO-bpy nanocomposite, (c) the emission spectra of Eu³⁺@UiO-bpy when excited by the wavelength at 340-370 nm, and (d) the *CIE* chromaticity coordinates calculated from the emission spectra shown in (c).

crystal sizes of ~100 nm (Figure 1c). N_2 adsorption measurements performed on bpy-UiO at 77 K revealed a type I adsorption isotherm with a pore volume of 1.12 cm^3 g^{-1} (Figure S1). The BET and Langmuir surface areas are 2258 m^2 g^{-1} and 3430 m^2 g^{-1}, respectively.

It is well established that bipyridyl group can coordinate with lanthanides and serve as 'antenna' for sensitizing the luminescence of lanthanides.[9c,14] Bipyridyl moieties of bpy ligands are embedded as free Lewis basic sites in bpy-UiO, thus we reasoned that they can act as scaffolds to anchor and sensitize lanthanide cations (Figure 1a). Bearing this in mind, bpy-UiO was immersed in methanol solution of chlorine salt of Eu³⁺ to afford Eu³⁺@bpy-UiO composite. PXRD pattern of Eu³⁺@bpy-UiO was identical to that of the pristine bpy-UiO, indicating that the crystallinity of bpy-UiO was maintained in Eu³⁺@bpy-UiO (Figure 1b). TEM image showed that the morphology and size of bpy-UiO were barely changed upon the incorporation of Eu³⁺ (Figure 1d). The Eu³⁺ loading of the Eu³⁺@bpy-UiO was determined as 2.1% by inductively coupled plasma-mass spectrometry (ICP-MS) analyses of Zr/Eu ratios of the digested MOF composite. Eu³⁺@bpy-UiO is very stable, and the incorporated Eu³⁺ cations can't leach into solutions during the adsorption of VOCs, which suggests that Eu³⁺ are incorporated within framework indeed by the strong coordination interaction between Eu³⁺ and free bipyridyl moieties. This was further verified by the photoelectron spectroscopy (XPS) studies (Figure S2). The Eu 4d peak position of MOF composite shifted to a lower region in comparison with that of $EuCl_3$. In addition, the N1s peak from free bipyridyl nitrogen atoms at 395.5 eV in bpy-UiO shifted to 396.4 eV upon incorporation of Eu³⁺, revealing the binding of bipyridyl moieties to Eu³⁺ in Eu³⁺@bpy-UiO. N_2 adsorption-desorption isotherm of Eu³⁺@bpy-UiO is shown in Figure S1. As expected, Eu³⁺@bpy-UiO shows reduced values of BET (1553 m^2 g^{-1}) and Langmuir surface (2242 m^2 g^{-1}) in comparison with bpy-UiO. TG analysis revealed that Eu³⁺@bpy-UiO is thermally stable to 450 °C, above which a weight loss of 57.1 wt% is attributed to decomposition of the framework (Figure S3).

The photoluminescence spectra of bpy-UiO and Eu³⁺@bpy-UiO were examined at room temperature in solid state (Figure 2). Upon excitation at 380 nm, the pristine bpy-UiO exhibits a strong broad
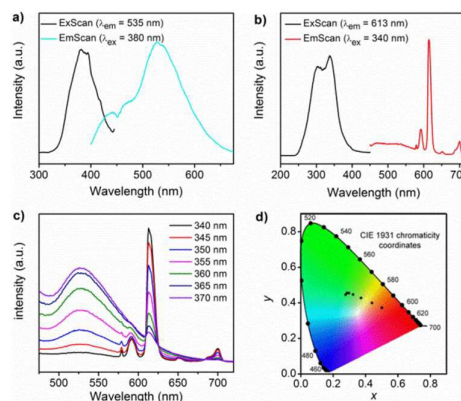
band centered at 535 nm, which can be attributed to the π–π* electron transition of organic linkers (Figure 2a). After the incorporation of Eu³⁺ cations, as expected, the MOF nanocomposite shows characteristic sharp Eu³⁺ emission bands at 590, 613, 653, and 701 nm, which are ascribed to the $^5D_0 \rightarrow ^7F_J$ (J = 1-4) transitions of Eu³⁺ (Figure 2b), respectively. The Eu³⁺ luminescence is mainly sensitized by the organic linkers within the parented framework. Such ligand-to-Eu³⁺ energy transfer behaviors have been confirmed by the excitation spectrum of Eu³⁺@bpy-UiO monitored at 613 nm, which displays an intense broad band peaking at 340 nm. The luminescence lifetime ($^5D_0 \rightarrow ^7F_2$) and quantum yield of the MOF composite are determined as respective 0.471 ms and 11.3%, which is reasonably high and can comparable with the lanthanides incorporated MOF counterpart.[15]

As Eu³⁺@bpy-UiO presents two emitters in the visible range, bpy ligand and Eu³⁺, we reasoned that such a MOF composite enables us to systematically tune the emission color by modulating the excitation wavelength. Figure 2c shows the emission spectra Eu³⁺@bpy-UiO with excitation wavelengths from 340 to 370 nm. The intensity of the broad ligand emission increases with excitation wavelength varying from 340 to 370 nm, while the Eu³⁺ emission recedes in the meantime. As the emission color of Eu³⁺@bpy-UiO is balanced on the synergetic contribution from Eu³⁺ and bpy ligand dual emission, the change in the intensity ratio of Eu³⁺ emission and bpy ligand emission will result in different emission colors. As shown in Fig. 2d, the chromaticity coordinates calculated from the emission spectra (Figure 2c) shifts from the red region to the cyan region. The emission colors observed by naked eye are in good agreement with the calculated chromaticity (Figure S4).

Given the emission intensities of bpy and Eu³⁺ are comparable when excited at 355 nm, the 355 nm excitation wavelength was employed to explore the capability of Eu³⁺@bpy-UiO nanocomposite in volatile organic compounds (VOCs) sensing. A class of aromatic VOCs was introduced into the channels of the activated Eu³⁺@bpy-UiO by exposure to different solvents, such as benzene, toluene, o-xylene, m-xylene, p-xylene, ethylbenzene, chlorobenzene, and benzonitrile. Unlike the other MOF systems displaying guest induced-fit structural transformation,[12a,j,16]
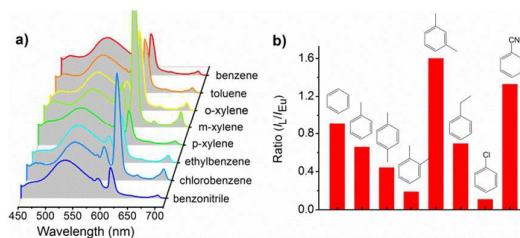
Figure 3 The emission spectra (a) and I_L/I_{Eu} intensity ratios (b) of Eu^{3+}@UiO-bpy after the encapsulation of different armoatic VOCs. The emission spectra (λ_{ex} = 355 nm) are normalized to the intensity of the ligand emission.

Eu^{3+}@bpy-UiO retained a rigid and stable framework after adsorbing different VOCs, as indicated by the almost same PXPD patterns of Eu^{3+}@bpy-UiO and the VOCs included samples (Figure S5). Figure 3a presents the emission spectra of Eu^{3+}@bpy-UiO after different VOCs accommodation. The spectra were normalized to the intrinsic ligand-based emission intensity of the framework. It is noted that the MOF composite shows sensitive ratiometric luminescence responses toward various VOCs. The intensity ratio of the ligand-based emission to Eu^{3+} emission (I_L/I_{Eu}) significantly depends on the included VOCs. Compared with the pristine Eu^{3+}@bpy-UiO, the VOCs incorporated MOF composite exhibits different degrees of variation in intensity ratio (I_L/I_{Eu}). Among them, the p-xylene included Eu^{3+}@bpy-UiO has the largest I_L/I_{Eu}. Moreover, the ratiometric luminescence of Eu^{3+}@bpy-UiO is highly responsive to different concentrations of VOCs and Mixed VOCs (Figure S6-8). The ratiometric luminescence response rate of Eu^{3+}@bpy-UiO toward VOCs is very fast, as illustrated by the time-dependent emission spectra of Eu^{3+}@bpy-UiO by exposure to m-xylene (Figure 9).Since the emission energy of Eu^{3+} is mainly transferred from the bpy ligand excitation, and the energy transfer processes might be tuned by guest accommodation through host-guest interactions, such a unique guest-dependent change in ratiometric luminescence is most likely attributed to the influence of the encapsulation of VOCs within the MOF on the energy transfer efficiency from the bpy ligand to the incorporated Eu^{3+} cations.[12i-k,17] Furthermore, the luminescence decay time ($^5D_0 \rightarrow {}^7F_2$) of Eu^{3+}@bpy-UiO substantially changed upon adsorption of different VOCs (Figure S10), which supports that ratiometric luminescence responses towards VOCs can be rationalized by the guest-dependent energy transfer from bpy ligands to Eu^{3+} cations. In addition to the ratiometric luminescence changes, peak shifts can be observed in ligand emission of Eu^{3+}@bpy-UiO upon adsorption of aromatic VOCs (Table S1). Given the pyridine rings should have only a small energy barrier associated with rotation away from the coplanar configuration, it is highly possible that the peak shifts are caused by the conformation change of free pyridine rings of Eu^{3+}@bpy-UiO exposed to the adsorbed VOCs.

The ratiometric luminescence responses of Eu^{3+}@bpy-UiO nanocomposite toward different VOCs can be exploited to differentiate these VOCs with similar structure and physical properties. As shown in Figure 3b, there is a one-to-one correspondence between the resulting I_L/I_{Eu} and the encapsulated VOCs. Although the values of I_L/I_{Eu} in toluene and ethylbenzene included samples are relatively close, it still can be distinguished by a modern fluorescence spectrometer which can measured a 0.02%

change of intensity ratio. Therefore, these VOCs can be readily decoded by monitoring the ratiometric emission intensity (I_L/I_{Eu}) of the host MOF composite. Such a self-referencing strategy can circumvent the complications existed in intensity measurement of a single emission, such as the errors introduced by optical occlusion, concentration inhomogeneities, excitation power fluctuations, or environment-induced nonradiative relaxation, thus is more accurate and reliable.

In addition, the luminescence quantum yield of the Eu^{3+}@bpy-UiO nanocomposite is also responsive to the accommodation of VOCs. As shown in Figure S11, the presence of VOCs increases quantum yield distinctly compared to that of the pristine Eu^{3+}@bpy-UiO. For example, a quantum yield of 27.4% was achieved in benzonitrile loaded Eu^{3+}@bpy-UiO, which is much higher than that of the pristine MOF nanocomposite (11.3%). The above observation reveals that the interaction between bpy ligands and the incorporated VOCs may hinder the vibration/rotation of pyridine rings to reduce the nonradiative decay processes.[12a,b] Notably, the accommodation of different VOCs has different effects on quantum yield of Eu^{3+}@bpy-UiO, providing an indication that these VOCs can also be distinguished by monitoring the luminescence quantum yield.

To maximizing the available information and enhancing the power of VOCs recognition, we proposed a dual-readout orthogonal identification scheme. The new orthogonal identification scheme was demonstrated in connection to both the emission intensity ratio (I_L/I_{Eu}) and quantum yield of the Eu^{3+}@bpy-UiO nanocomposite. Since the information of the VOCs can be carried by the ratiometric emission intensity and luminescence quantum yield (Φ) of the VOCs included Eu^{3+}@bpy-UiO, each of the VOCs relates with one unique two-dimensional (2D) readout (I_L/I_{Eu}, Φ). The 2D readouts were arranged in a decoded map (Figure 4). These readouts are well separated and identified in the decoded map, suggesting that one can precisely differentiate these VOCs through a ratiometric emission intensity & luminescence quantum yield-dual readout process. For example, we randomly selected one among these analyte aromatic VOCs to encapsulate into Eu^{3+}@bpy-UiO nanocomposite, and the 2D readouts (I_L/I_{Eu}, Φ) of the VOC incorporated sample was determined as (0.922, 0.178), so that the VOC could be recognized as benzene (Figure S12). In theory, with adequate VOCs being tested, a database of the 2D readouts (I_L/I_{Eu}, Φ) can be established, which provide a standard to identify an unknown VOC. However, it is difficult to check the simple rule for the theoretical relationship between I_L/I_{Eu} and quantum yield of the
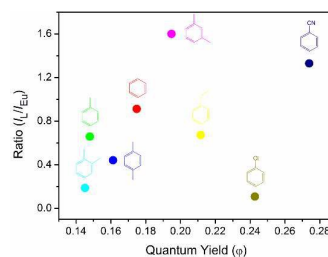
Figure 4 A 2D decoded map of the aromatic VOCs based on the emission intensity ratio (I_L/I_{Eu}) and quantum yield (Φ) responses of Eu^{3+}@bpy-UiO nanocomposite toward the VOCs accommodation.

COMMUNICATION

VOCs incorporated Eu^{3+}@bpy-UiO. The intensity ratio of bpy ligand and Eu^{3+} emission (I_L/I_{Eu}) significantly depends on the energy transfer efficiency from bpy ligands to Eu^{3+} cations, while the overall quantum yield of Eu^{3+}@bpy-UiO nanocomposite is contributed by both bpy ligand and Eu^{3+} emission. Thus, to understand theoretical relationship between I_L/I_{Eu} and quantum yield of the VOCs incorporated Eu^{3+}@bpy-UiO needs much further deep studies on the complicated radiative or nonradiative transition processes in Eu^{3+}@bpy-UiO nanocomposite.

The reusability of Eu^{3+}@bpy-UiO nanocomposite in sensing VOCs was tested by recycling experiments (Figure S13). We measured the emission spectra and luminescence quantum yield of three cycles of Eu^{3+}@bpy-UiO ↔ Eu^{3+}@bpy-UiO⊃benzonitrile (immersing and desolvating), and no significant change in ratiometric emission intensity and luminescence quantum yield was observed. It suggests that the Eu^{3+}@bpy-UiO nanocomposite is recyclable for decoding VOCs. Besides, the good regeneration performance of the MOF nanocomposite implies that the interaction between the host framework and the guest VOCs are indeed weak, and the reversion of luminescence and quantum yield of the framework is due to the removal of VOCs.

In summary, a responsive luminescent MOF nanocomposite was developed for the recognition of aromatic VOCs with similar structures and physical properties. The VOCs recognition was based on an unprecedented dual-readout orthogonal identification scheme, which is demonstrated in connection with the ratiometric emission intensity (I_L/I_{Eu}) and luminescence quantum yield (Φ) of the MOF nanocomposite. Since the photoluminescence properties (I_L/I_{Eu}, Φ) of the MOF nanocomposite highly depend on the VOCs accommodation, identities regarding these analytes VOCs can be decoded into a corresponding 2D readout (I_L/I_{Eu}, Φ). This novel dual-readout identification scheme is capable of maximizing the available information, thus is expected to be more reliable and powerful in chemical sensing in comparison with the conventional emission intensity-based strategy. With adequate VOCs being tested, a database of the 2D readouts might be established, which provide a standard to identify an unknown VOC.

Notes and references

1 (*a*) J. He, M. Zeller, A. D. Hunter and Z. Xu, *J. Am. Chem. Soc.*, 2012, **134**, 1553; (*b*) C. Y. Sun, X. L. Wang, X. Zhang, C. Qin, P. Li, Z. M. Su, D. X. Zhu, G. G. Shan, K. Z. Shao, H. Wu and J. Li, *Nat. Commun.*, 2013, **4**, 2717; (*c*) D. F. Sava, L. E. S. Rohwer, M. A. Rodriguez and T. M. Nenoff, *J. Am. Chem. Soc.*, 2012, *134*, 3983; (d) Y. Zhou and B. Yan, *Nanoscale*, 2015, **7**, 4063.

2 (*a*) Z. C. Hu, B. J. Deibert and J. Li, *Chem. Soc. Rev.*, 2014, **43**, 5815; (*b*) Y. J. Cui, B. L. Chen and G. D. Qian, *Coord. Chem. Rev.*, 2014, **273**, 76; (*c*) X. J. Zhang, W. J. Wang, Z. J. Hu, G. N. Wang and K. S. Uvdal, *Coord. Chem. Rev.*, 2015, **284**, 206.

3 (*a*) Y. T. Li, J. L. Tang, L. C. He, Y. Liu, Y. L. Liu, C. Y. Chen and Z. Y. Tang, *Adv. Mater.*, 2015, **27**, 4075; (*b*) K. M. L. Taylor-Pashow, J. Della Rocca, Z. G. Xie, S. Tran and W. B. Lin, *J. Am. Chem. Soc.*, 2009, **131**, 14261; (*c*) A. C. McKinlay, R. E. Morris, P. Horcajada, G. Ferey, R. Gref, P. Couvreur and C. Serre, *Angew. Chem., Int. Edit.*, 2010, **49**, 6260.

4 (*a*) K. A. White, D. A. Chengelis, K. A. Gogick, J. Stehman, N. L. Rosi and S. Petoud, *J. Am. Chem. Soc.*, 2009, **131**, 1806; (*b*) Q. Y. Yang, M. Pan, S. C. Wei, K. Li, B. B. Du and C. Y. Su, *Inorg. Chem.*, 2015, **54**, 5707; (*c*) Y. Zhou and B. Yan, *J. Mater. Chem. C*, 2015, **3**, 8413.

5 (*a*) Y. Zhou, H. H. Chen and B. Yan, *J. Mater. Chem. A*, 2014, **2**, 13691; (*c*) J. N. Hao and B. Yan, *Chem. Commun.*, 2015, **51**, 7737.

6 (*a*) H. Xu, C. S. Cao and B. Zhao, *Chem. Commun.*, 2015, **51**, 10280; (*b*) B. L. Chen, L. B. Wang, F. Zapata, G. D. Qian and E. B. Lobkovsky, *J. Am. Chem. Soc.*, 2008, *130*, 6718.

7 (*a*) Y. Li, S. S. Zhang and D. T. Song, *Angew. Chem. Int. Edit.*, 2013, **52**, 710; (*b*) Y. L. Hou, H. Xu, R. R. Cheng and B. Zhao, *Chem. Commun.*, 2015, **51**, 6769; (*c*) S.Y. Zhang, W. Shi, P. Cheng, and M. J. Zaworotko, *J. Am. Chem. Soc.*, 2015, **137**, 12203.

8 (*a*) Z. S. Dou, J. C. Yu, Y. J. Cui, Y. Yang, Z. Y. Wang, D. R. Yang and G. D. Qian, *J. Am. Chem. Soc.*, 2014, **136**, 5527; (*b*) P. Y. Wu, J. Wang, C. He, X. L. Zhang, Y. T. Wang, T. Liu and C. Y. Duan, *Adv. Funct. Mater.*, 2012, **22**, 1698.

9 (*a*) Y. J. Cui, R. J. Song, J. C. Yu, M. Liu, Z. Q. Wang, C. D. Wu, Y. Yang, Z. Y. Wang, B. L. Chen and G. D. Qian, *Adv. Mater.*, 2015, **27**, 1420; (*b*) Z. P. Wang, D. Ananias, A. Carne-Sanchez, C. D. S. Brites, I. Imaz, D. Maspoch, J. Rocha and L. D. Carlos, *Adv. Funct. Mater.*, 2015, **25**, 2824; (*c*) Y. Zhou, B. Yan and F. Lei, *Chem. Commun.*, 2014, **50**, 15235;

10 (*a*) H. L. Jiang, D. W. Feng, K. C. Wang, Z. Y. Gu, Z. W. Wei, Y. P. Chen and H. C. Zhou, *J. Am. Chem. Soc.*, 2013, **135**, 13934; (*b*) H. Y. Li, Y. L. Wei, X. Y. Dong, S. Q. Zang and T. C. W. Mak, *Chem. Mater.*, 2015, **27**, 1327; (*c*) J. Aguilera-Sigalat and D. Bradshaw, *Chem. Commun.*, 2014, **50**, 4711.

11 A. Douvali, A. C. Tsipis, S. V. Eliseeva, S. Petoud, G. S. Papaefstathiou, C. D. Malliakas, I. Papadas, G. S. Armatas, I. Margiolaki, M. G. Kanatzidis, T. Lazarides and M. J. Manos, *Angew. Chem., Int. Edit.*, 2015, **54**, 1651;

12 (*a*) Y. Takashima, V. M. Martinez, S. Furukawa, M. Kondo, S. Shimomura, H. Uehara, M. Nakahama, K. Sugimoto and S. Kitagawa, *Nat. Commun.*, 2011, *2*,168; (*b*) M. Zhang, G. X. Feng, Z. G. Song, Y. P. Zhou, H. Y. Chao, D. Q. Yuan, T. T. Y. Tan, Z. G. Guo, Z. G. Hu, B. Z. Tang, B. Liu and D. Zhao, *J. Am. Chem. Soc.*, 2014, **136**, 7241; (*c*) J. H. Wang, M. Li and D. Li, *Chem. Sci.*, 2013, **4**, 1793; (*d*) Z. C. Hu, K. Tan, W. P. Lustig, H. Wang, Y. G. Zhao, C. Zheng, D. Banerjee, T. J. Emge, Y. J. Chabal and J. Li, *Chem. Sci.*, 2014, **5**, 4873; (*e*) X. G. Liu, H. Wang, B. Chen, Y. Zou, Z. G. Gu, Z. J. Zhao and L. Shen, *Chem. Commun.*, 2015, **51**, 1677; (*f*) Y. X. Guo, X. Feng, T. Y. Han, S. Wang, Z. G. Lin, Y. P. Dong and B. Wang, *J. Am. Chem. Soc.*, 2014, **136**, 15485; (*g*) J. L. Chen, F. Y. Yi, H. Yu, S. H. Jiao, G. S. Pang and Z. M. Sun, *Chem. Commun.*, 2014, **50**, 10506; (*h*) F. Y. Yi, Y. Wang, J. P. Li, D. Wu, Y. Q. Lan and Z. M. Sun, *Mater. Horiz.*, 2015, **2**, 245; (*i*) D. P. Yan, Y. Q. Tang, H. Y. Lin and D. Wang, *Sci. Rep.*, 2014, *4*; (*j*) M. J. Dong, M. Zhao, S. Ou, C. Zou and C. D. Wu, *Angew. Chem., Int. Edit.*, 2014, **53**, 1575; (*k*) C. Zhan, S. Ou, C. Zou, M. Zhao and C. D. Wu, *Anal. Chem.*, 2014, **86**, 6648; (*l*) R. Haldar, R. Matsuda, S. Kitagawa, S. J. George and T. K. Maji, *Angew. Chem., Int. Edit.*, 2014, **53**, 11772.

13 L. J. Li, S. F. Tang, C. Wang, X. X. Lv, M. Jiang, H. Z. Wu and X. B. Zhao, *Chem. Commun.*, 2014, **50**, 2304.

14 K. Binnemans, *Chem. Rev.*, 2009, **109**, 4283.

15 (*a*) J. Y. An, C. M. Shade, D. A. Chengelis-Czegan, S. Petoud and N. L. Rosi, *J. Am. Chem. Soc.*, 2011, **133**, 1220; (*b*) Y. Q. Lan, H. L. Jiang, S. L. Li and Q. Xu, *Adv. Mater.*, 2011, **23**, 5015; (*c*) Y. Zhou and B. Yan, *Inorg. Chem.*, 2014, **53**, 3456.

16 (*a*) G. Férey, C. Serre, *Chem. Soc. Rev.* 2009, *38*, 1380; (*b*) S. Horike, S. Shimomura, S. Kitagawa, *Nat. Chem.* 2009, **1**, 695.

17 J. M. Zhou , H. H. Li , H. Zhang , H. M. Li , W. Shi , and P. Cheng, *Adv. Mater.*, 2015, **27**, 7072.